

Phase stability of Ti_3SiC_2 at high pressure and high temperature

Jiaqian Qin^{a,*}, Duanwei He^b

^a*Metallurgy and Materials Science Research Institute, Chulalongkorn University, Bangkok 10330, Thailand*

^b*Institute of Atomic and Molecular Physics, Sichuan University, Chengdu 610065, PR China*

Received 24 January 2013; received in revised form 29 April 2013; accepted 29 April 2013

Available online 22 May 2013

Abstract

Phase stability of Ti_3SiC_2 was studied under high pressure and high temperature using X-ray diffraction, scanning electron microscopy, and energy-dispersive X-ray spectroscopy. From the results obtained, the decomposition temperature of Ti_3SiC_2 decreases quickly against pressure, and the low temperature limits of phase segregation of the sample Ti_3SiC_2 lie between 1100 °C and 1000 °C, 1000 °C and 900 °C, 900 °C and 800 °C, under high pressures of 3, 4 and 5 GPa, respectively. Ti_3SiC_2 decomposes to generate TiC, SiC, and TiSi_x . On the basis of the experimental results, we suggest two decomposition models to explain the phase decomposition of Ti_3SiC_2 at high pressure and high temperature. © 2013 Elsevier Ltd and Techna Group S.r.l. All rights reserved.

Keywords: Ti_3SiC_2 ; Decomposition; High pressure and high temperature

1. Introduction

Ti_3SiC_2 , a layered ternary carbide, belongs to the $\text{M}_{n+1}\text{AX}_n$ (MAX) compounds, where $n=1, 2$ or 3 , M is an early transition metal, A is an A-group element, and X is C or N [1–3]. The MAX phase materials such as Ti_2AlC , Ti_2AlN , Ti_3AlC_2 and Ti_3SiC_2 possess potential applications as engineering materials due to its low density, high-elastic modulus, high-thermal conductivity, and good machinability [1–3].

The MAX phases exhibit a hexagonal structure (space group $\text{P6}_3/\text{mmc}$). In Ti_3SiC_2 , Ti_3C_2 layers (isostructural to the binary TiC phase, where C is at octahedral sites) are intercalated with atomic layers of Si, which act as mirror planes [4]. The Si–Ti bonds are very weak, whereas the covalent Ti–C bonds are much stronger [3,5]. Ti_3SiC_2 exhibits unusual mechanical properties and chemical stability at high temperatures [3,6–11]. Barsoum et al. have reported that Ti_3SiC_2 was stable and did not decompose after annealing in vacuum at temperatures as high as 1600 °C. Furthermore, Ti_3SiC_2 bulk material was found to be thermally stable in Ar atmosphere up to at least 1800 °C, but its resistance to carburization appears to be poor [7–12]. Recently, it has been reported that Ti_3SiC_2 is stable up to 61 GPa at room temperature based on synchrotron X-ray diffraction

measurements [13,14]. However, $\beta\text{-Ti}_3\text{SiC}_2$, another polymorph of Ti_3SiC_2 within the same space group $\text{P6}_3/\text{mmc}$, has been identified by high-resolution electron microscopy observations [15,16], and Sun et al. [17] reported that Ti_3SiC_2 exhibits two polymorphs in which Si shifts from 2b to 2d (Wyckoff position) at approximately 700 °C.

Most recently, Emmerlich et al. [18] reported that the Ti_3SiC_2 thin films maintain their stability during annealing at temperatures up to ~1000 °C for 25 h, but annealing at 1100–1200 °C results in the rapid decomposition of Ti_3SiC_2 by Si outward-diffusion along the basal planes via domain boundaries to the free surface with subsequent evaporation. These results are in apparent contrast to the reported decomposition temperatures for bulk material at 1800–2300 °C [7–12].

MAX phases are expected to be used in harsh environments of high stress and high temperature such as automobile and aircraft engine components, rocket engine nozzles, aircraft brakes, and racing car brake pads and discs, so it is interesting to look at their behavior at simultaneous high pressure and high temperature conditions. In our previous work [19,20], we have reported that Ti_2AlC decomposes to generate titanium carbide and titanium aluminum after treated at high pressure and high temperature, and the decomposition temperature of Ti_2AlC decreases against pressure. Extensive studies show that Ti_3SiC_2 possesses potential for various applications and there is a growing interest in thin films of Ti_3SiC_2 as electrical contacts [21]. The role of the

*Corresponding author. Tel.: +66 2218 4234; fax: +66 2611 7586.

E-mail addresses: jiaqian.q@chula.ac.th, jiaqianqin@gmail.com (J. Qin).

environment is as important to the decomposition activation of Ti_3SiC_2 [10,22]. Therefore, there is a need to determine the potential phase decomposition in applications environments such as high pressure and high temperature conditions.

2. Experiments

The polycrystalline samples were fabricated by reactive hot pressing of Ti, SiC, and graphite powders at 1600 °C for 4 h under a pressure of 40 MPa. The synthesized sample was pulverized to powder (averaged grain size $\sim 3\text{ }\mu\text{m}$) and the X-ray diffraction pattern of the starting material is shown in Fig. 1(a). Besides the main phase of Ti_3SiC_2 , the starting samples also contain a minor phase of TiC. The purity of the Ti_3SiC_2 powder is estimated to be larger than 98% according to the examination. The powder was pre-compressed ($\sim 200\text{ MPa}$) into discs (8 mm diameter and 4 mm height). The starting sample discs were placed into hexagonal boron nitride capsules for treatments.

High pressure and high temperature experiments were carried out with a DS6 \times 8MN cubic press, and the experimental details were described elsewhere [19,20,23,24]. The sample temperature in the high-pressure cell was measured directly using a PtRh6%–PtRh30% thermocouple. The cell pressure is estimated by the oil pressure reading, which was calibrated by the melting of silver at high pressure. The sample was first pressurized to desired pressure, and then heated to high temperature with a heating rate of $\sim 350\text{ }^\circ\text{C/min}$. After keeping the high pressure–temperature conditions for 20 or 60 min, the samples were quenched to room temperature with cooling rates of about $100\text{ }^\circ\text{C/min}$ and then decompressed to ambient pressure. The treated samples were usually well sintered. All the recovered samples were carefully grinded and polished before examined by X-ray diffraction (XRD, DX-2500, Dandong, China), scanning electron microscopy (SEM, model JSM-6490, JEOL, Japan), and energy-dispersive X-ray spectroscopy (EDS, EDAX, USA). Transmission electron microscopy (TEM) was conducted with a JEOL 3011 high-resolution electron microscope. TEM specimens were prepared on an ultrathin carbon film on a holey carbon support film, 400 mesh grid supplied by Ted Pella, Inc., that had been soaked in 0.5% PDDA.

3. Results and discussions

3.1. X-ray diffraction

Fig. 1(b) is an X-ray diffraction pattern of the selected sample heat treated in vacuum at 1300 °C for 20 min, which was used to study the thermal stability of the Ti_3SiC_2 phase. It can be seen that the sample treated in vacuum at 1300 °C for 20 min has a similar X-ray diffraction pattern to that of the starting material (Fig. 1(a)), no new peaks were observed. Based on X-ray diffraction data for the sample treated in vacuum at high temperature, we think that Ti_3SiC_2 can maintain stability at high temperatures, at least up to 1300 °C

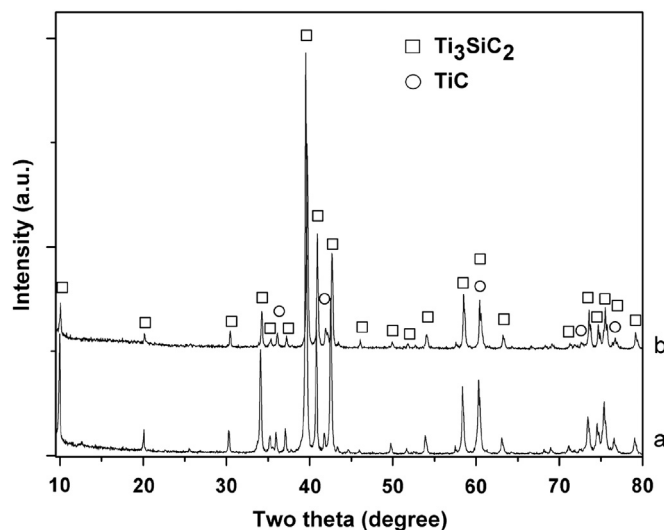


Fig. 1. (a) X-ray diffraction pattern of the starting materials and (b) X-ray diffraction pattern of the selected samples treated in vacuum at 1300 °C for 20 min to confirm the thermal stability of the Ti_3SiC_2 phase.

in vacuum. Our present result is in good agreement with the previous results [7–12].

Fig. 2 shows the X-ray diffraction patterns of the selected samples treated at high pressure–temperature conditions. There is no difference between the X-ray diffraction pattern of the high pressure and high temperature-treated sample at 5 GPa and 800 °C for 60 min (Fig. 2(a)) and that of the starting material (Fig. 1(a)). After the sample was treated at 5 GPa and 900 °C for 60 min as shown in Fig. 2(b), some new peaks were observed by X-ray diffraction, but we could not identify the new peaks from the X-ray diffraction data. It can be seen that the intensity of characteristic diffraction peaks of TiC (111) and TiC (200) increase (marked by arrow in Fig. 2(b)). The intensity of diffraction peaks of TiC and the new peaks was found to increase with increasing temperature for the samples treated at 5 GPa and high temperature above 900 °C. The X-ray diffraction data reveals that, Ti_3SiC_2 decomposes completely at 5 GPa and 1300 °C, and hence we can conclude that Ti_3SiC_2 decomposes to titanium carbide and unknown phase after heat treated at 5 GPa and high temperature. According to the X-ray diffraction data, we can calculate the lattice parameters of TiC ($a=4.3177\text{ }\text{\AA}$), which is very close to that of theoretical value ($a=4.322\text{ }\text{\AA}$, PDF #65-8804).

Samples were treated under pressures of 3 and 4 GPa at different temperatures and were also investigated in the same way. Some new peaks were also observed at high temperatures of 1000 °C and 1100 °C, under high pressure of 4 GPa and 3 GPa, respectively. The intensity of diffraction peaks of TiC and the new peaks was also found to increase with temperature. At pressures of 3, 4 and 5 GPa, the low temperature limits of phase segregation of the sample Ti_3SiC_2 lie between 1100 and 1000 °C, 1000 °C and 900 °C, 900 °C and 800 °C, respectively. Fig. 3 shows the P – T region of the phase segregation for Ti_3SiC_2 . It can be seen that the low temperature limits for the phase segregation for Ti_3SiC_2 strongly depend on the pressure.

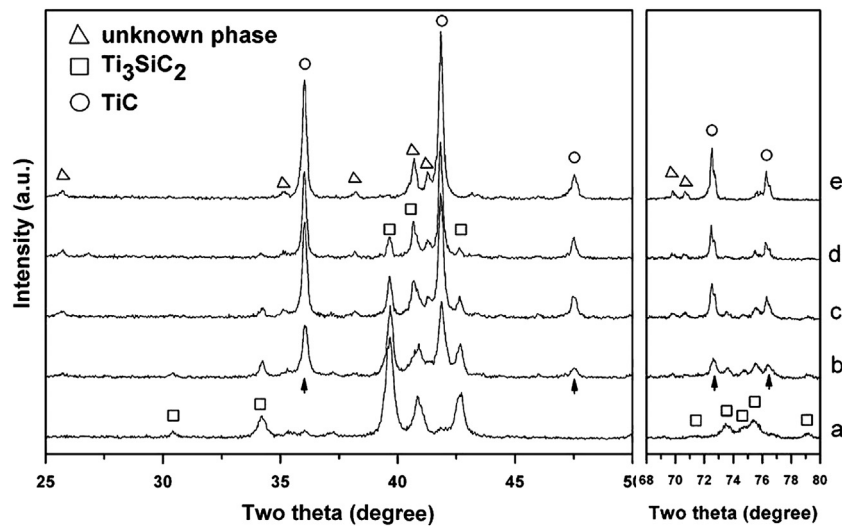


Fig. 2. X-ray diffraction patterns of the selected samples: (a) sample treated at 5 GPa and 800 °C for 60 min; (b) sample treated at 5 GPa and 900 °C for 60 min; (c) sample treated at 5 GPa and 1000 °C for 60 min; (d) sample treated at 5 GPa and 1200 °C for 20 min; and (e) sample treated at 5 GPa and 1300 °C for 20 min.

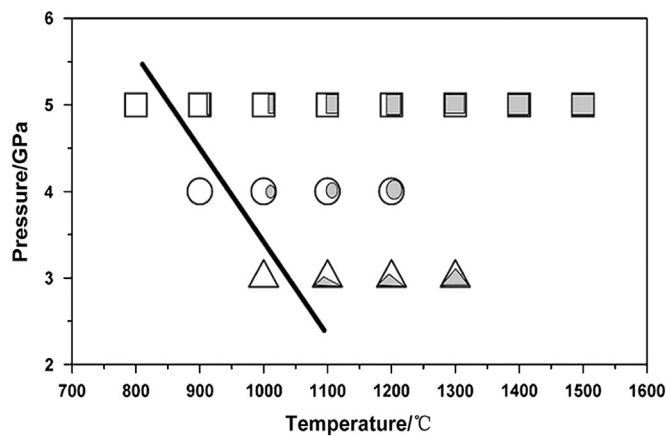


Fig. 3. P – T region of the phase segregation for the Ti_3SiC_2 (\square : 5 GPa, \circ : 4 GPa, and Δ : 3 GPa, the shadow areas to indicate decomposed).

The X-ray diffraction full width at half maximum (FWHM) values for the TiC (111) and TiC (200) peak is shown in Fig. 4 vs. temperature. For comparison, the full width at half maximum of starting materials was inserted into the figure. There is a sharp increase in the full width at half maximum from $\sim 0.208^\circ$ to $\sim 0.290^\circ$ for the TiC (111) peak and $\sim 0.138^\circ$ to $\sim 0.244^\circ$ for the TiC (200) peak when the Ti_3SiC_2 starts to decompose at 5 GPa and 900 °C. Since the full width at half maximum value is an inverse measure of crystallite size, the observed increase in full width at half maximum indicates the crystallite size refinement of TiC subsequent to the Ti_3SiC_2 decomposition under high pressure and high temperature, similar to those in the phase segregation of Ti_2AlC [19], are also revealed. This is followed by a distinct decrease of full width at half maximum to 0.2° for the TiC (111) peak and to 0.209° for the TiC (200) peak as temperature is raised to 1200 °C. The observed drop in full width at half maximum indicates that TiC layers recrystallize subsequent to the Ti_3SiC_2 decomposition.

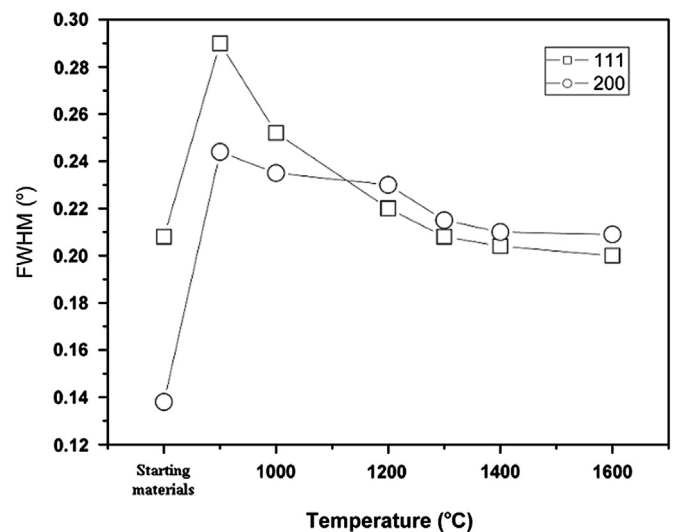


Fig. 4. The X-ray FWHM for the TiC (111) and TiC (200) peak during treating of Ti_3SiC_2 between 900 and 1600 °C under high pressure of 5 GPa. For comparison, the FWHM of starting materials were inserted into the figure.

3.2. Scanning electron microscopy and energy-dispersive X-ray spectroscopy

The X-ray diffraction patterns of the high pressure and high temperature-treated sample reveal some new peaks. Fig. 2(e) shows the X-ray diffraction pattern of the sample treated at 5 GPa and 1300 °C. According to the X-ray diffraction data, Ti_3SiC_2 has decomposed completely, and the treated sample contains TiC and unknown phase. To further confirm that the new peaks belong to the Ti–Si–C system, scanning electron microscopy and energy-dispersive X-ray spectroscopy were conducted. From the energy-dispersive X-ray spectroscopy results (Fig. 5), the starting material and the high pressure and high temperature-treated sample only contain Ti, Si, and C

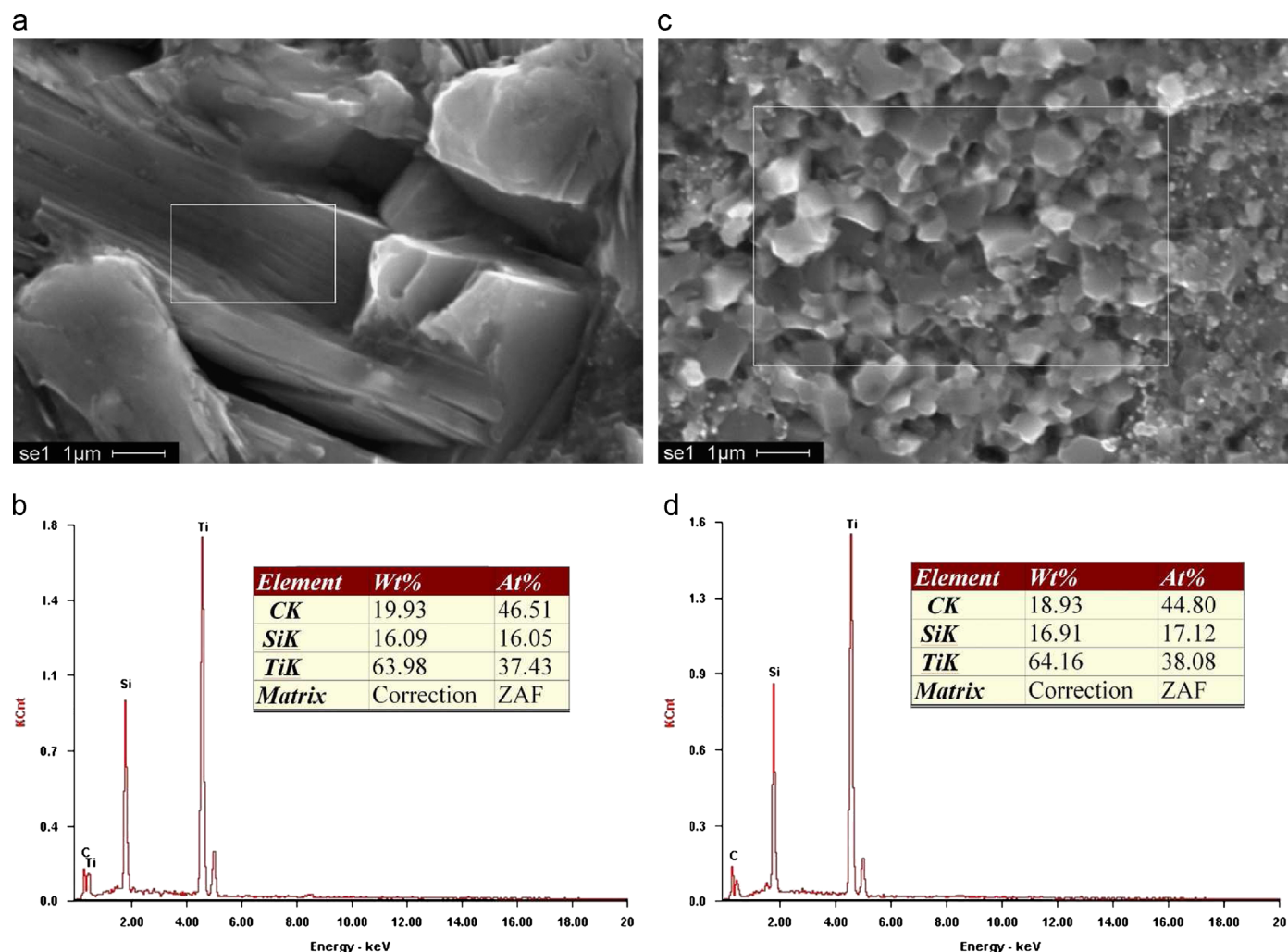


Fig. 5. Energy dispersive X-ray spectroscopy (EDS) of the starting material and the high pressure and high temperature-treated samples: (a,b) selected area and electron diffraction and EDS element analysis of starting material and (c,d) selected area and electron diffraction and EDS element analysis of the high pressure and high temperature-treated sample.

elements. So we propose that the unknown phase still belong to the Ti–Si–C system.

The microstructure of the high pressure and high temperature-treated samples observed by scanning electron microscopy can be seen in Fig. 6. One of the samples was treated at 5 GPa and 600 °C for 60 min as shown in Fig. 6(a). Based on the X-ray diffraction results, the Ti_3SiC_2 did not start to decompose, below 800 °C, under high pressure of 5 GPa. It can be seen that the sample has a layered microstructure, and the average grain size is about 4 μm in length and 1 μm in thickness. Besides, there are some particles with average grain size about 1 μm. By energy-dispersive X-ray spectroscopy analysis, they were determined as TiC, which is consistent with the X-ray diffraction results in Fig. 1(a). Increasing the sintering temperature up to 1000 °C and 5 GPa for 60 min results in a layered microstructure of Ti_3SiC_2 and lots of TiC particles with size of about 100 nm embedded in a homogenous matrix of fine grains as shown in Fig. 6(b). Besides, Fig. 6(c) also shows presence of few grains with hexagonal microstructure. By energy-dispersive X-ray spectroscopy analysis, we confirm that only three elements Ti, Si and C were present in the sample. With

further increasing the sintering temperature to 1400 °C at 5 GPa, as shown in Fig. 6(d), the hexagonal microstructure material and the TiC particles were also observed, but no layered microstructure of Ti_3SiC_2 was observed from the scanning electron microscopy and energy-dispersive X-ray spectroscopy results. This concludes that, Ti_3SiC_2 has decomposed completely at 5 GPa and 1400 °C for 20 min, and the scanning electron microscopy and energy-dispersive X-ray spectroscopy results is in good agreement with the X-ray diffraction results. From the scanning electron microscopy (Fig. 6(d)) analysis, the average grain size of TiC is about 500 nm, and we also conclude that grain size refinement of TiC particles subsequent to the Ti_3SiC_2 decomposition under 1000 °C at 5 GPa, is a result of recrystallization due to further heat treatment to 1400 °C at 5 GPa. This result is also in accord with the full width at half maximum results (Fig. 4).

3.3. Transmission electron microscopy

To identify the unknown phase, the sample treated at 5 GPa and 1400 °C was also investigated by transmission electron

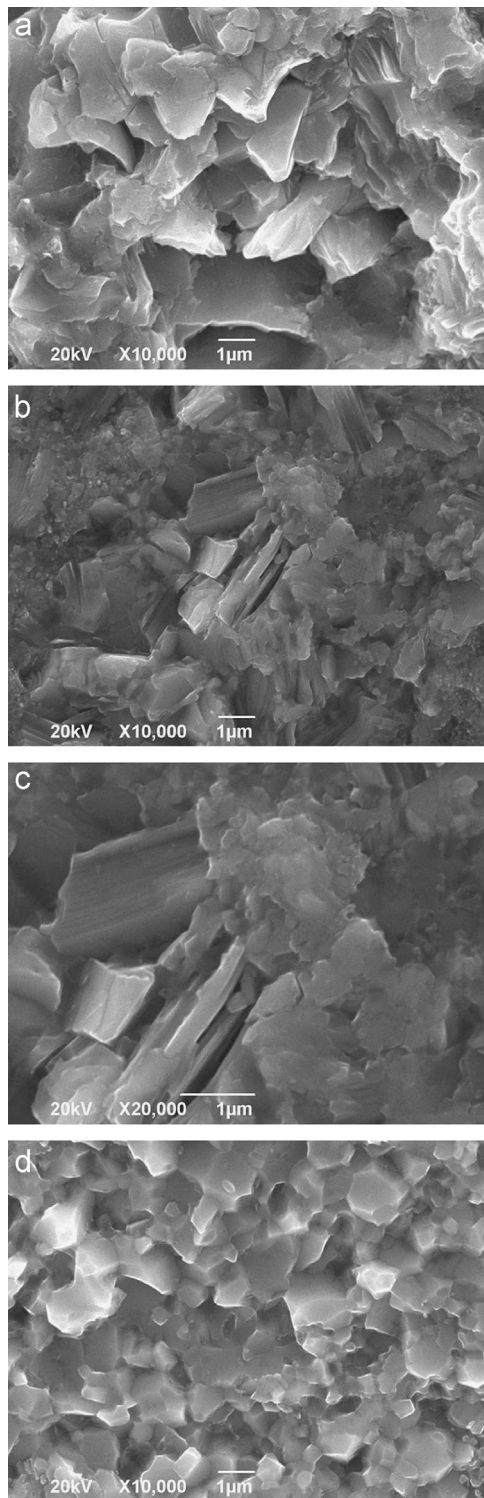


Fig. 6. SEM of the selected samples: (a) sample treated at 5 GPa and 600 °C for 60 min; (b) sample treated at 5 GPa and 1000 °C for 60 min; (c) the enlarged image of the selected area in (b); and (d) sample treated at 5 GPa and 1400 °C for 20 min.

microscopy. The microstructure of the sample treated at 5 GPa and 1400 °C shown in Fig. 7, and the selected area electron diffraction (SAED) patterns were inserted into Fig. 7. The SAED patterns could be indexed as the diffraction patterns of TiC

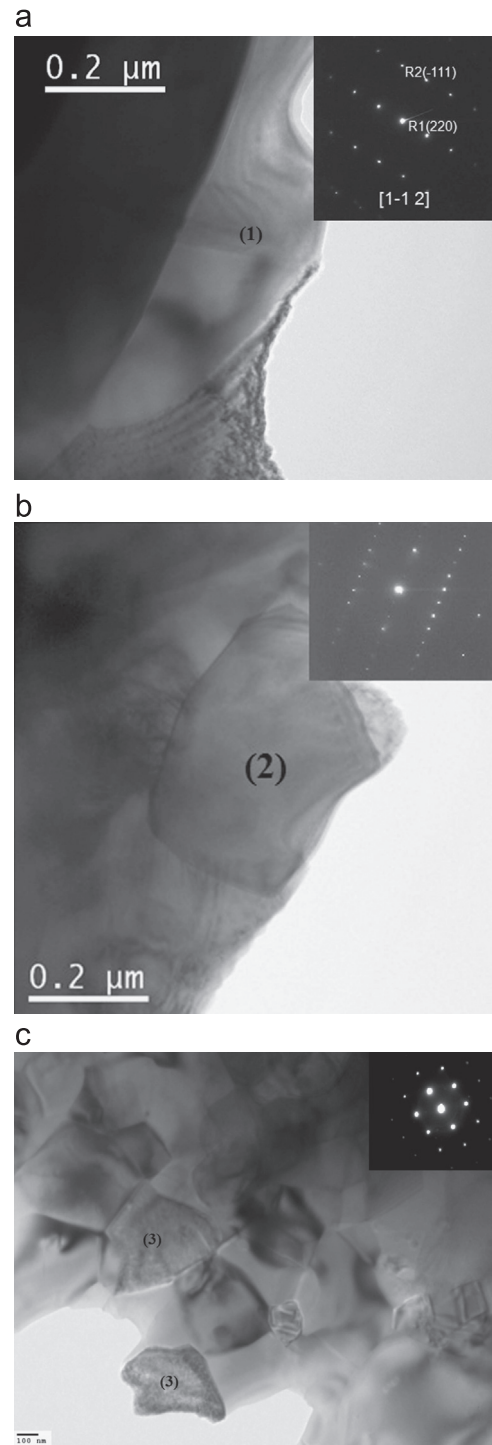


Fig. 7. TEM image of Ti_3SiC_2 treated at 5 GPa and 1400 °C with marked areas (1, 2, and 3) with SAED for phases present in the marked areas: (a) (1) TiC, (b) (2) SiC, and (c) (3) TiSi_x .

(Fig. 7a, point 1), SiC (Fig. 7b, point 2), and TiSi_x (Fig. 7c, point 3). The SAED patterns of TiC can be indexed as the diffraction patterns of $[1-12]$ zone axis of TiC, and the lattice parameter is $a=4.3 \text{ \AA}$, which is in good agreement with the X-ray diffraction results ($a=4.3177 \text{ \AA}$). Here we also showed the element maps, which are extremely useful for displaying element distributions in textural context, particularly for showing

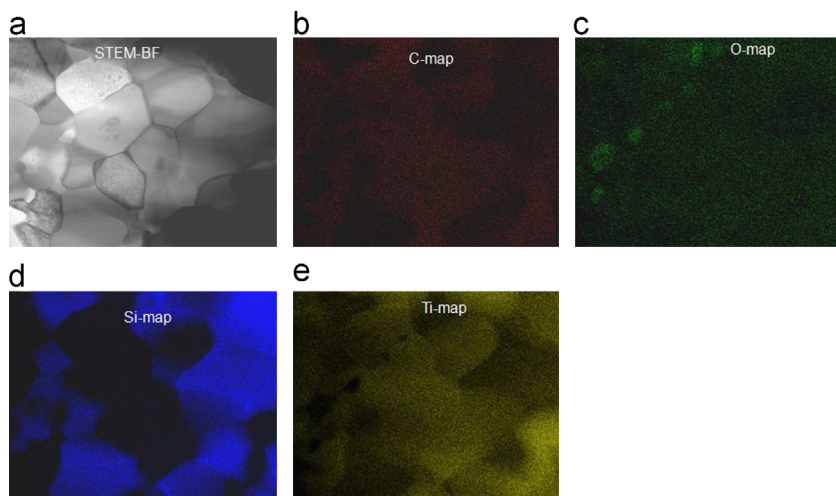


Fig. 8. (a) Bright-field STEM image of Ti_3SiC_2 treated at 5 GPa and 1400 °C and (b–e) X-ray mapping of various elements in STEM mode.

compositional zonation. Fig. 8 shows the bright-field scanning transmission electron microscopy (STEM-BF) images and the X-ray elemental mapping in the scanning transmission mode of the sample treated at 5 GPa and 1400 °C. It is clear from the image that the sample contains Ti, Si, and C element, and the phases of TiC, SiC, and TiSi_x could be deduced from color overlay. Such observations were also supported by SAED results.

Recently, Emmerlich et al. [18] reported that Ti_3SiC_2 (0001) thin films are effectively stable during vacuum furnace annealing up to 1100 °C, above which they decompose into TiC_x ($x \sim 0.67$) following outward diffusion of Si and then its evaporation. However, the high pressure and high temperature experiment could be considered as an approximate enclosed space, and we conclude that Ti_3SiC_2 decomposes to TiC, SiC, and TiSi_x after high pressure and high temperature synthesis, which was confirmed by XRD, TEM, SAED, and X-ray elemental mapping. Therefore we think the reported decomposition model [18] does not accord with our present high pressure and high temperature experiment. The energy-dispersive X-ray spectroscopy results of the high pressure and high temperature-treated samples reveals presence of Si elements, so Si evaporation was unlikely to take place in the enclosed space. On the basis of the experimental results, we suggest two decomposition models to explain the phase decomposition of Ti_3SiC_2 .

Model I: As the Si–Ti bonds are very weak, whereas the covalent Ti–C bonds being much stronger [3,5], we think that the outward diffusion of Si was also likely to take place in our high pressure and high temperature experiment and the material shrinks by the relaxation of the Ti_3C_2 slabs, similar to those observed in Ti_3SiC_2 thin films phase decomposition [18]. However, no Ti_3C_2 or $\text{TiC}_{0.67}$ phase was observed by X-ray diffraction. During the relaxation process because of the redistribution of C atoms [18], Si is likely to react with Ti_3C_2 or $\text{TiC}_{0.67}$ and form TiC, SiC, and TiSi_x at high pressure–temperature conditions.

Model II: As the long-range atomic rearrangement becomes more difficult due to the compression, the outward diffusion of

Si may be very difficult under high pressure. We think Ti_3SiC_2 will directly decompose to TiC, SiC, and TiSi_x at high pressure and high temperature.

As mentioned above, our experimental results show that the external compression can lower the decomposition temperature of Ti_3SiC_2 , similar to that observed in Ti_2AlC phase segregation [19,20]. However, the long-range atomic rearrangement in case of Ti_2AlC becomes more difficult due to the compression. This may be the reason that no phase transformations were observed up to 61 GPa in the previous studies [13,14]. In this work and our previous studies [19,20], phase segregation of both Ti_3SiC_2 and Ti_2AlC have been observed at simultaneous high pressure and high temperature conditions, indicating that a suitable high temperature is needed to dynamically make the phase segregate at high pressure for Ti_3SiC_2 and Ti_2AlC . This result confirms that the environment plays the dominant role in the decomposition activation of Ti_3SiC_2 [10,22].

4. Conclusions

In summary, we find that Ti_3SiC_2 is unstable under high pressure and high temperature; the decomposition temperature of Ti_3SiC_2 decreases quickly against pressure, and the low temperature limits of phase segregation of the sample Ti_3SiC_2 lie between 1100 °C and 1000 °C, 1000 °C and 900 °C, 900 °C and 800 °C, under high pressures of 3, 4 and 5 GPa, respectively. The observed onset for the Ti_3SiC_2 decomposition under HPHT is in apparent contrast to the reported decomposition temperatures for bulk material in the range of 1800–2300 °C [8,12]. We conclude that the discrepancy in the decomposition temperature is in part a result of the difference in the high pressure-high temperature environments between the studies. The role of the environment is thus important to the decomposition activation of Ti_3SiC_2 [10,22].

According to XRD, TEM, SAED, and X-ray elemental mapping results, Ti_3SiC_2 decomposes to generate TiC, SiC, and TiSi_x after the samples were treated at high pressure and high temperature. On the basis of the experimental results, we

suggest two decomposition models to explain the phase decomposition of Ti_3SiC_2 at high pressure and high temperature.

Acknowledgments

The authors gratefully acknowledge Dr. Kai Sun of University of Michigan for TEM analysis. JQ would like to acknowledge support from Metallurgy and Materials Science Research Institute (NO. MMRI PP/1/2556) and Chulalongkorn University (No. GDNS 56-010-62-001).

References

- [1] M.W. Barsoum, A. Murugaiah, S.R. Kalidindi, T. Zhen, Kinking non-linear elastic solids, nanoindentations, and geology, *Physical Review Letters* 92 (2004) 255508-1–255508-4.
- [2] M.W. Barsoum, T. El-Raghy, The MAX phases: unique new carbide and nitride materials, *American Scientist* 89 (2001) 334–343.
- [3] M.W. Barsoum, The MN+1AX_n phases: a new class of solids; thermodynamically stable nanolaminates, *Progress in Solid State Chemistry* 28 (2000) 201–281.
- [4] W. Jeitschko, H. Nowotny, Die Kristallstruktur von Ti_3SiC_2 —ein neuer Komplexcarbide-Typ, *Monatshefte für Chemie* 98 (1967) 329–337.
- [5] R. Ahuja, O. Eriksson, J.M. Wills, B. Johansson, Electronic structure of Ti_3SiC_2 , *Applied Physics Letters* 76 (2000) 2226–2228.
- [6] Z. Sun, Y. Zhou, J. Zhou, The anomalous flow behaviour in the layered Ti_3SiC_2 ceramic, *Philosophical Magazine Letters* 80 (2000) 289–293.
- [7] M.W. Barsoum, T. El-Raghy, Synthesis and characterization of a remarkable ceramic: Ti_3SiC_2 , *Journal of the American Ceramic Society* 79 (1996) 1953–1956.
- [8] R. Radhakrishnan, J.J. Williams, M. Akinc, Synthesis and high-temperature stability of Ti_3SiC_2 , *Journal of Alloys and Compounds* 285 (1999) 85–88.
- [9] M.W. Barsoum, T. El-Raghy, M. Radovic, Ti_3SiC_2 : a layered machinable ductile ceramic, *Interceram* 49 (2000) 226–233.
- [10] C. Racault, F. Langlais, R. Naslain, Solid-state synthesis and characterization of the ternary phase Ti_3SiC_2 , *Journal of Materials Science* 29 (1994) 3384–3392.
- [11] J. Lis, Y. Miyamoto, R. Pampuch, K. Tanihata, Ti_3SiC_2 -based materials prepared by HIP-SHS techniques, *Materials Letters* 22 (1995) 163–168.
- [12] Y. Du, J.C. Schuster, H. Seifert, F. Aldinger, Investigation and thermodynamic calculation of the titanium–silicon–carbon system, *Journal of the American Ceramic Society* 83 (2000) 197–203.
- [13] A. Onodera, H. Hirano, T. Yuasa, N.F. Gao, Y. Miyamoto, Static compression of Ti_3SiC_2 to 61 GPa, *Applied Physics Letters* 74 (1999) 3782–3784.
- [14] J.L. Jordan, T. Sekine, T. Kobayashi, X. Li, N.N. Thadhani, T. El-Raghy, M.W. Barsoum, High pressure behavior of titanium–silicon carbide Ti_3SiC_2 , *Journal of Applied Physics* 93 (2003) 9639–9643.
- [15] L. Farber, I. Levin, M.W. Barsoum, T. El-Raghy, T. Tzenow, High-resolution transmission electron microscopy of some $\text{Ti}_{n+1}\text{AX}_n$ compounds ($n=1, 2$; $\text{A}=\text{Al}$ or Si ; $\text{X}=\text{C}$ or N), *Journal of Applied Physics* 86 (1999) 2540–2543.
- [16] R. Yu, Q. Zhan, L.L. He, Y.C. Zhou, H.Q. Ye, Polymorphism of Ti_3SiC_2 , *Journal of Materials Research* 17 (2000) 948–950.
- [17] Z. Sun, J. Zhou, D. Music, R. Ahuja, J.M. Schneider, Phase stability of Ti_3SiC_2 at elevated temperatures, *Scripta Materialia* 54 (2006) 105–107.
- [18] J. Emmerlich, D. Music, P. Eklund, O. Wilhelmsson, U. Jansson, J.M. Schneider, H. Högborg, L. Hultman, Thermal stability of Ti_3SiC_2 thin films, *Acta Materialia* 55 (2007) 1479–1488.
- [19] J. Qin, D. He, C. Chen, J. Wang, J. Hu, B. Yang, Phase segregation of titanium–aluminium carbide (Ti_2AlC) at high pressure and high temperature, *Journal of Alloys and Compounds* 462 (2008) L24–L27.
- [20] J. Qin, D. He, L. Lei, P. An, L. Fang, Y. Li, F. Wang, Z. Kou, Differential thermal analysis study of phase segregation of Ti_2AlC under high pressure and high temperature, *Journal of Alloys and Compounds* 476 (2009) L8–L10.
- [21] H.L. Tuller, M.A. Spears, R. Mlcak, United States Patent No. US 2002/0068 488 A1, 2002.
- [22] M.W. Barsoum, T. El-Raghy, L. Farber, M. Amer, R. Christini, A. Adams, The topotactic transformation of Ti_3SiC_2 into a partially ordered cubic $\text{Ti}(\text{C}_{0.67}\text{Si}_{0.06})$ phase by the diffusion of Si into molten cryolite, *Journal of the Electrochemical Society* 146 (1999) 3919–3923.
- [23] C. Chen, D. He, Z. Kou, F. Peng, L. Yao, R. Yu, Y. Bi, B_6O -based composite to rival polycrystalline cubic boron nitride, *Advanced Materials* 19 (2007) 4288.
- [24] J. Qin, D. He, J. Wang, L. Fang, L. Lei, Y. Li, J. Hu, Z. Kou, Y. Bi, Is rhenium diboride a superhard material?, *Advanced Materials* 20 (2008) 4780–4783.